ELSEVIER
Available online at www.sciencedirect.com
ScienceDirect
Procedia Engineering 10 (2011) 1133–1138
Engineering Procedia

ICM11

Mixed Mode 3D Stress Fields and Crack Front Singularities for Surface Flaw

V.N.Shlyannikov[a], A.V.Tumnov[a]

[a]*Research Center for Power Engineering Problems of the Russian Academy of Sciences, Lobachevsky Street 2/31, Kazan 420111, Russia*

Abstract

The elastic-plastic stress fields and mode mixity parameters for semi-elliptical surface cracks on biaxial loaded plates have been investigated using detailed three-dimensional finite element calculations. Different degrees of mode mixity are given by combinations of the far-field stress level, biaxial stress ratio and inclined crack angle. For a wide range of crack inclination angles, elastic-plastic stress fields along the crack front for both semi-circular and semi-elliptical surface cracks being subjected to remote biaxial loading have been obtained. For both crack geometry types, it was demonstrated that, in the vicinity of the corner, the behavior stress fields differ from the stress component distributions at the deepest point on the crack front. This phenomenon is due to the free surface effect. Combining analytical solutions and 3D finite element calculations, the elastic crack tip singularity for a surface semi-elliptical crack has been investigated on a biaxially loaded plate. The distributions of singularity exponents have been obtained along the crack front for three main cases of mixed-mode loading.

Selection and peer-review under responsibility of ICM11

Keywords: Inclined semi-elliptical crack, load biaxiality, crack tip singularity

1. Introduction

Surface flaws are typical damage to different types of engineering structures. The assessment of changes in both the form and the size of the surface cracks during propagation is an essential element for the prediction of the structural integrity of biaxially loaded engineering structures, such as pressured vessels and pipelines in the presence of initial and accumulated operation damages. Frequently in practice, inclined cracks are encountered and accurate assessment of the fracture resistance under monotonic loading or the remaining fatigue life for such problems requires one to account for the geometrically induced mode mixity, i.e., the non-normal crack in the loading direction. Therefore three-

* Corresponding author. Tel.: +7 843 231 90 20 ; fax:+7 843 231 90 20
E-mail address: shlyannikov@mail.ru

1877-7058 © 2011 Published by Elsevier Ltd. Open access under CC BY-NC-ND license.
Selection and peer-review under responsibility of ICM11 doi:10.1016/j.proeng.2011.04.187

dimensional solutions obtained for biaxially loaded plates containing inclined surface flaws can generally be very useful in assessing the fracture conditions in the given problem of interest.

2. Computational procedures

Three-dimensional finite elements are used to model a plate containing a semi-elliptical surface crack. The geometry and coordinate system used are shown in Fig. 1. The finite element analyses are performed using ANSYS. A finite element mesh consisting of 224 elements placed along curvilinear crack front. In the circumferential direction, 40 equally sized elements are defined in the angular region from 0 to π. A finite element mesh consisting of 1,144,530 nodes and 275,784 twenty-node quadrilateral brick elements was used. The FEA calculations in this work are based on the J_2 incremental theory of plasticity. The Ramberg-Osgood model was employed to define the stress-strain curve corresponding to the elastic-plastic material properties. For all of our analyses, the hardening coefficient n = 4.96 and α =3, the Young's modulus E=206 GPa, the yield stress σ_y = 380 MPa, and the Poisson's ratio ν=0.3 were used.

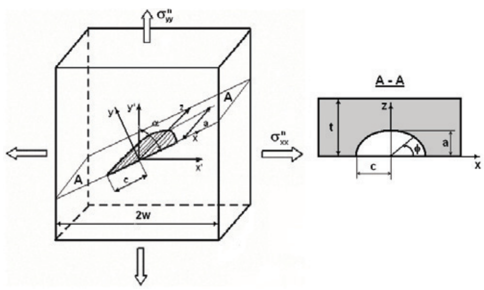

Fig. 1. A semi-elliptical inclined surface crack in a plate under remote uniform biaxial loading

The three-dimensional finite element data have been used to determine the elastic-plastic stress component angular distributions along the surface crack front for different load biaxialities. Some results for both semi-circular ($\varepsilon = 1.0$) and semi-elliptical ($\varepsilon = 0.5$) surface cracks which were subjected to remote equi-biaxial tension ($\eta = +1$, $\alpha = \pi/2$) and equi-biaxial tension-compression loading ($\eta = -1, \alpha = \pi/4$), are given in Fig. 2; they have dimensionless hoop stress $\tilde{\sigma}_{\theta\theta}$ and both in-plane $\tilde{\sigma}_{\rho\theta}$ and out-of-plane $\tilde{\sigma}_{\theta\omega}$ shear stresses. Remarkably, all angular stress distributions are symmetrical with respect to the crack plane $\theta = 0^\circ$ under the considered loading conditions. As can be seen from Fig. 2, both mode I hoop stress $\tilde{\sigma}_{\theta\theta}$ and mode III out-of-plane shear stress $\tilde{\sigma}_{\theta\omega}$ increase along the surface semi-elliptical crack front when the angle is altered from $\bar{\varphi} = 0$ (the free surface) to $\bar{\varphi} = 1.0$ (the deepest point). The elastic-plastic dimensionless mode II in-plane stress $\tilde{\sigma}_{\rho\theta}$ decreases due to the out-of-plane effect, and it equals zero as the deepest point is approached along the crack front. The effect of the corner singularity on all full field stress components is also evident in Fig. 2. Nevertheless, the free surface fields ($\varphi = 0$) are distinctly different from the two-dimensional plane stress field, which is due to the significance of the strong out-of-plane stress gradients.

The dimensionless angular stress component distributions are given in Fig. 3 as functions of the crack inclination angle ($2\alpha/\pi$) for the semi-elliptical ($\varepsilon = 0.5$) surface crack, which is subjected to remote equi-biaxial tension-compression loading ($\eta = -1$). This loading variant was selected because particular cases contain the pure mode I ($\alpha = \pi/2$), pure mode II ($\alpha = \pi/4, \varphi = 0$) and pure mode III ($\alpha = \pi/4$,

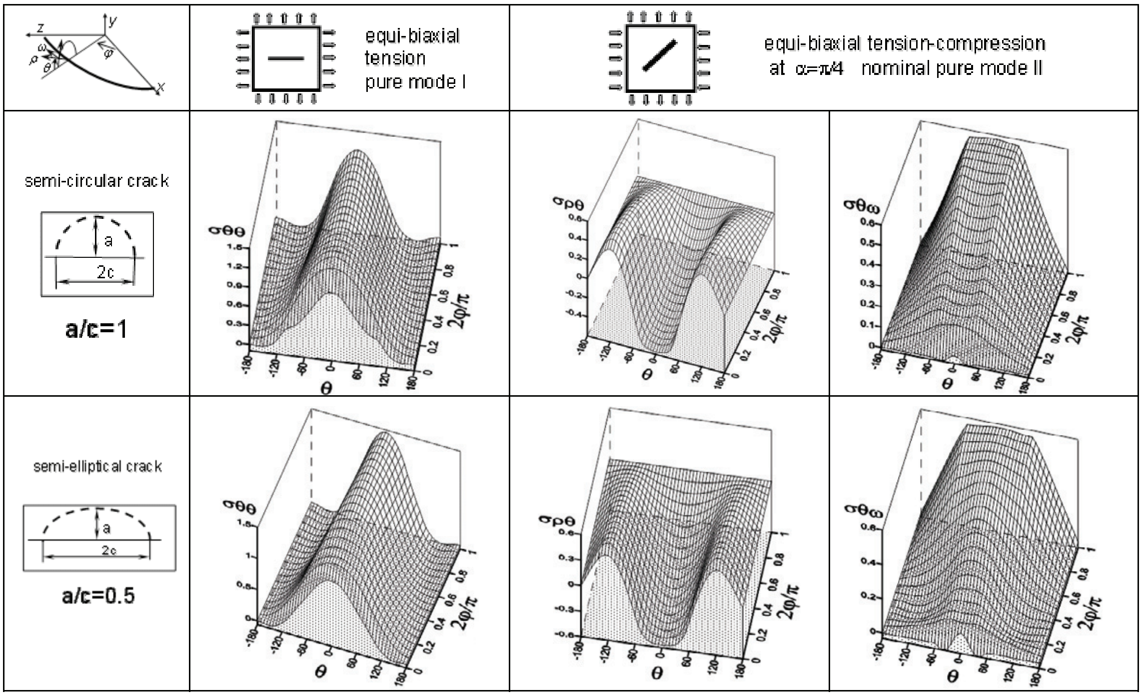

Fig. 2. Angular stress distributions along crack front of semi-circular and semi-elliptical cracks

$\varphi = \pi/2$) at the surface semi-elliptical crack. Note that the angular stress distributions for the dimensionless crack tip distance r/l = 0.01 (where l = 5 mm) are given in Fig. 3. Additionally, equi-biaxial tensile-compression loading is analyzed at a large number of different values of inclination of the angle α. Although the loads acting at the ends of the plate are uniform tensile-compression pressure loads, the problems exhibit mixed-mode fracture conditions due to different values of the inclination angle. The elastic-plastic stress fields on the free surface shown in Fig. 3(a,b,c) may be compared to the stress fields in the deepest point of the crack front, as shown in Fig. 3(d,e,f). Fig. 3(a) shows that, for the semi-elliptical surface flaw geometry (ε =0.5) and on the free surface under equi-biaxial tension-compression loading ($\eta = -1$), the angular hoop stress distribution takes its maximum value at $2\alpha/\pi = 1$ in the crack plane at the polar angle θ =0°. It also decreases towards an inclination angle value of $2\alpha/\pi = 0.5$. After having moved from the pure mode I $2\alpha/\pi = 1$ a symmetrical-type distribution of the hoop stress because of a decreasing inclination angle α, the angular stress field at $2\alpha/\pi = 0.5$ reaches an anti-symmetrical type that corresponds to the pure mode II for a given parametrical angle of ellipse φ = 0°. Unlike this situation, in the deepest point of the crack front $\varphi = \pi/2$, the hoop stress distribution in Fig. 3(d) preserved a tendency to return to a symmetrical type because it decreased its maximum value's magnitude and, finally, $\tilde{\sigma}_{\theta\theta}$ equaled zero for any θ at $2\alpha/\pi = 0.5$. Contrary to that behavior, the in-plane shear stress $\tilde{\sigma}_{\rho\theta}$ in Fig. 3(b) on the free surface changed from an anti-symmetrical type at $2\alpha/\pi = 1$ with decreases of the crack inclination angle to a symmetrical distribution with respect to the crack plane θ =0° for $2\alpha/\pi = 0.5$. In the deepest point of the crack front, as shown in Fig.3 (e), the in-plane shear stress $\tilde{\sigma}_{\rho\theta}$ decreases as the inclination angle decreases, and it equals zero for any θ at $2\alpha/\pi = 0.5$.

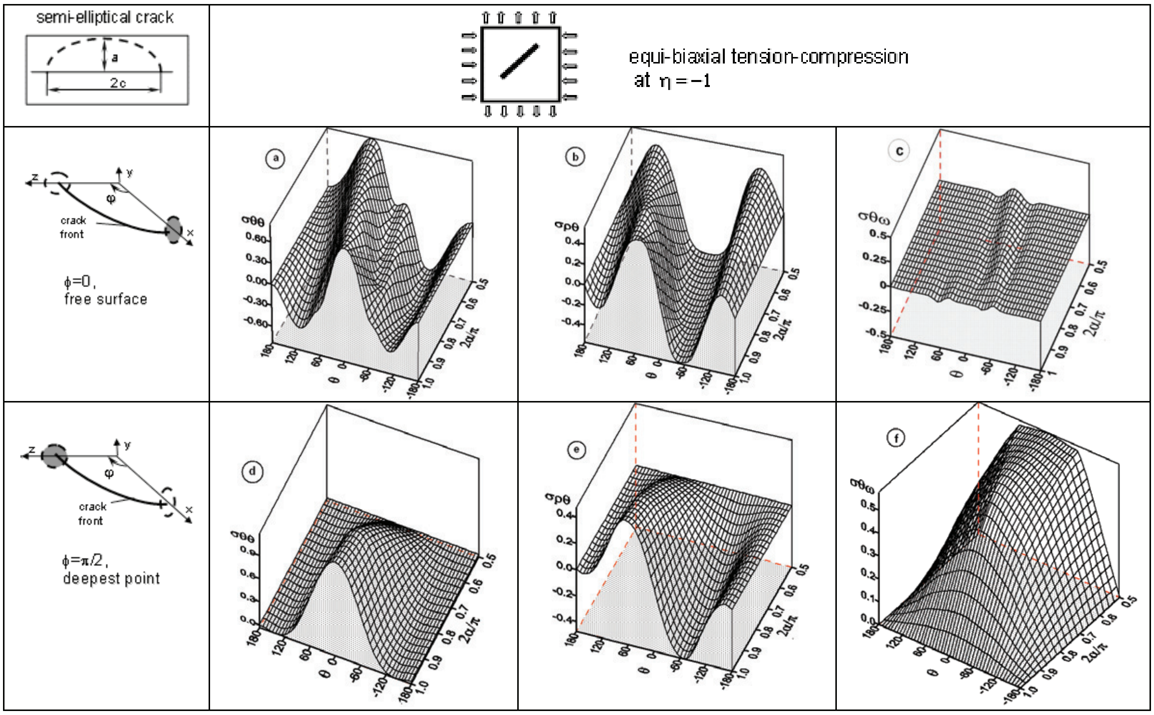

Fig. 3. Angular stress distributions as a function of crack inclination angle

Qualitatively $\widetilde{\sigma}_{\rho\theta}$ decreases as the inclination angle decreases, and it equals zero for any θ at $2\alpha/\pi = 0.5$. Qualitatively similar behavior of both the hoop and the in-plane shear stresses on the free surface of the plate with a semi-elliptical crack was mentioned by Shlyannikov [1] for through-thickness mixed cracks. On the free surface of the plate at φ = 0 when $\eta = -1$, $2\alpha/\pi = 0.5$ takes place in the mixed mode II+III, while for the same values of $\eta = -1$ and $2\alpha/\pi = 0.5$ in the deepest point of the crack front at $\varphi = \pi/2$, the pure mode III conditions are realized. This is because both the hoop stress and the in-plane shear stress are equal to zero, but the out-of-plane shear stress takes its maximum value with a symmetrical type of angular distribution, as follows from Fig. 3(f).

3. Crack-tip singularity

Under general elastic stressing, the stress field along the interior points of the crack front is the superposition of the conventional modes I, II and III, which are characterized by an inverse square root dependence on the distance from the tip. At the point where the crack front intersects the free surface, a three-dimensional corner singularity exists and its effect on the mode I, II and III stress intensity factor distributions is apparent. We analyzed such far field mixed-mode loading conditions when the non-singular T-stress is equal to zero, i.e., when the first term in the elastic stress expansion is under equi-biaxial tension ($\eta = +1$) and equi-biaxial tension-compression ($\eta = -1$) with the crack inclination angle $\alpha = \pi/4$. We consider and use the following stress expansion in the form of equations of Eftis and Subramonian [2]:

$$\sigma_{ij} = K_i r^{\lambda} \tilde{\sigma}_{ij}^{REF}(\theta) + T\delta_{1i}\delta_{1j}, \quad \text{where} \quad T = \sigma_{yy}^{n}(1-\eta)\cos 2\alpha. \tag{1}$$

In Eqs. (1), r and θ correspond to the local polar coordinates measured from the periphery of the crack front in the plane perpendicular to it (Fig. 1). Also $\tilde{\sigma}_{ij}^{REF}(\theta)$ are the well known dimensionless angular stress functions, σ_{yy}^{n} is the nominal stress in the y-axis direction, $\eta = \sigma_{xx}^{n}/\sigma_{yy}^{n}$ is the nominal stress biaxial ratio and α is the inclined crack angle. The solution for arbitrary uniform remote biaxial stressing of an inclined surface crack (Fig. 1) is obtained by the substitution of the appropriate full field FEA stresses $\sigma_{ij} = \sigma_{ij}^{FEM}$ into Eq. (1). The stress intensity factors for modes I, II and III of a surface semi-elliptical crack in Eq. (1) can be calculated from the general equation

$$K_i = \sigma_i^{\infty}\sqrt{\pi \cdot l}, \qquad l = 1\Big/\sqrt{(\cos\varphi/c)^2 + (\sin\varphi/a)^2} \tag{2}$$

In this equation l is the current crack length. The remote stresses related to the nominal biaxial stress σ_{yy}^{n} are defined as

$$\sigma_I^{\infty} = \sigma_{yy}^{n}\left(\cos^2\alpha + \eta\sin^2\alpha\right), \quad \sigma_{II}^{\infty} = \sigma_{yy}^{n}\frac{1-\eta}{2}\sin 2\alpha\cos\varphi, \quad \sigma_{III}^{\infty} = \sigma_{yy}^{n}\frac{1-\eta}{4}\sin 2\alpha\sin\varphi. \tag{3}$$

A particular case of pure mode I at equi-biaxial tension is realized when $\eta = +1$ and in this case, Eq. (1) implies T=0. By substituting the dimensionless angular functions at θ=0° into Eq. (4) are found to be

$$\lambda_1 = \ln\left(K_1/\sigma_{\theta\theta}^{FEM}\right)/\ln(2\pi r). \tag{4}$$

A particular case of equi-biaxial tension-compression is realized when $\eta = -1$ and $\alpha = \pi/4$, and in this case, Eq.(1) again implies T=0. In an analogous way, the crack tip singularities for sub-problems II and III are derived from the local stress field on the plane where θ=0°:

$$\lambda_2 = \frac{\ln\left[\frac{1}{\sigma_{\rho\theta}^{FEM}}\left(K_{II}\cos\varphi + K_{III}\sin\varphi\right)\right]}{\ln(2\pi r)}, \quad \lambda_3 = \frac{\ln\left[\frac{1}{\sigma_{\theta\omega}^{FEM}}\left(K_{III}\cos\varphi - K_{II}\sin\varphi\right)\right]}{\ln(2\pi r)}. \tag{5}$$

The crack tip singularity directly ahead of the crack plane at *θ=0°* is calculated by using Eqs.(4) and (5) for the three-dimensional field in which biaxial loading is only based on the elastic stress intensity factor (when *T=0*). These singularities are shown in Fig. 4. Under pure elastic conditions, this results in a corner field, which does not exhibit the familiar two-dimensional $r^{-1/2}$ stress singularity. This theoretical finding is confirmed by crack tip singularity distributions along the crack front in Fig. 4. Compared to the in-plane shear stress distribution at the deepest point of the crack front in Fig. 3e, the FEA results in Fig. 4 show that the crack tip singularity λ_2 is close to zero when $\tilde{\sigma}_{\rho\theta}$-stress disappears at $\eta = -1$ and $\alpha = \pi/4$. This feature is also shown on the free surface by a three-dimensional field in Fig. 3c, when the out-of-plane shear stress $\tilde{\sigma}_{\theta\omega}$-stress disappears at $\eta = -1$ and $\alpha = \pi/4$ and the crack tip singularity λ_3 becomes close to zero in Fig. 4. It follows from Fig. 4 that the effective zone of dominance of the inverse square root behavior of the crack tip singularity comprises a very small fraction of the crack front. The crack-front singularity of the mode I field λ_1 is stronger, and those of the in-plane λ_2 and out-of-plane λ_3 shear modes II and III are weaker functions of the crack tip distance, which have absolute values r that are normalized by the crack length a. Comparing the crack-front distributions for the semi-circular surface

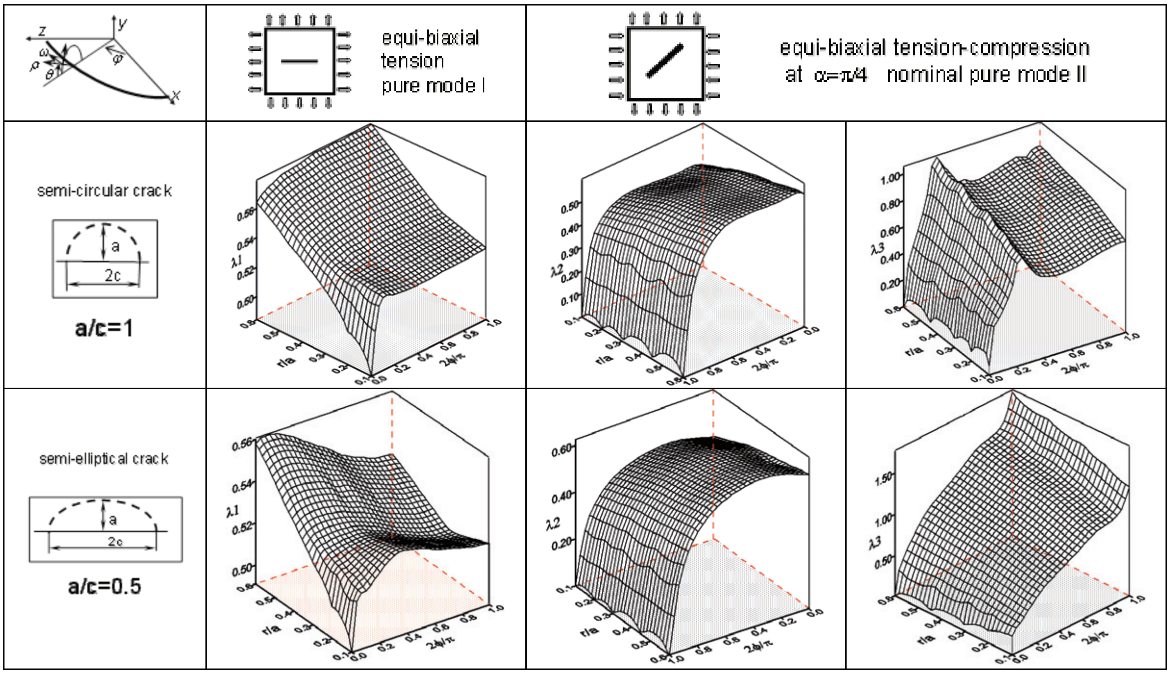

Fig. 4. Elastic crack tip singularity behavior along crack front

crack to the ones for the semi-elliptical crack clearly shows the influence of the surface flaw shape on the singularity behavior under different mixed modes of loading.

4. Conclusions

The elastic-plastic stress fields and crack front singularity parameters for semi-elliptical surface crack have been investigated in biaxial loaded plates by detailed three-dimensional finite element calculations. The influence of aspect ratio of the semi-elliptical surface flaw, the biaxial loading and the initial crack angle on both elastic and plastic stress components distributions are discussed. In all situations, it is found that the behavior of stress fields along a curvilinear crack front strongly depends on the crack-front position described by the parametrical semi-ellipse angle. In the particularly case of a pure shear nominal stress state, the stress fields changed from pure mode II near the border of the semi-elliptical surface crack to pure mode III at the deepest point of crack front. These analyses were performed for different surface flaw geometries to study the combined load biaxiality and mode mixity effects on the crack-front stress fields and the size and shape of the plastic zones.

Numerical method of singular parameters determination is suggested accounting for first term of asymptotic expansion. Crack-tip singularity parameters behavior for particular cases of the equi-biaxial tension and the equi-biaxial tension-compression are presented. It was shown for both semi-circular and semi-elliptical crack types, that the load biaxiality has a principal effect on the crack front singularity.

References

[1] ShlyannikovVN. Elastic-plastic mixed-mode fracture criteria and parameters. Springer-Verlag: Berlin; 2003.
[2] Eftis J, Subramonian N. The inclined crack under biaxial load. Engineering Fracture Mechanics 1978; 10; 43-67.